Brain Research, 555 (1991) 10–18

ADONIS 000689939116813T

BRES 16813

Thalamically projecting cells of the lateral cervical nucleus in monkey

Mark V. Smith and A. Vania Apkarian

Neurosurgery Research Laboratories, SUNY Health Science Center, 3118 Weiskotten Hall, Syracuse, NY 13210 (U.S.A.)

(Accepted 26 February 1991)

Key words: Horseradish Peroxidase; Spinal cord; *Macaca*; *Saimiri*; Cell count

The number, location, and morphology of thalamically projecting lateral cervical nucleus (LCN) cells were determined in monkey using retrograde transport of wheatgerm agglutinin-conjugated horseradish peroxidase. These data were compared to the total population of LCN neurons as determined by Nissl stain. In 4 *Macaca fascicularis* and one *Saimiri sciureus* the average size of the thalamic projection from LCN was found to be 506 ± 94 cells contralateral to the injections. Thalamically projecting LCN neurons were located between the lower medulla and the third cervical segment; approximately 90% of these cells were in the first two cervical segments. Morphologic analysis of thalamically projecting LCN cells showed that they were smaller in size, and more oblong in shape in caudal regions of the nucleus. In 3 macaques, the average total number of LCN cells was determined to be 1617 ± 908 on one side, in Nissl material. In these Nissl-stained preparations LCN neurons were found as far caudal as the fourth cervical segment; 68% were located in the first two cervical segments. Hence, thalamically projecting LCN neurons in the monkey are located in the rostral portion of the nucleus and comprise about one-third of the total population. Comparison of these data with reports in the literature imply that, unlike the cat, the major projection from LCN in monkeys is to the mesencephalon rather than to the thalamus.

INTRODUCTION

The lateral cervical nucleus (LCN) is located within the dorsolateral funiculus of the upper cervical spinal cord. This nucleus is part of a spino-cervico-thalamic pathway which receives projections from ipsilateral spinal cord neurons with axons located in the dorsolateral[4,12,15,21,23,30,45,49] and dorsal funiculi[24,42]. Spinocervical tract neurons are located in ipsilateral laminae III and IV throughout the spinal cord in cats, rats and dogs[4,16,21], and in laminae IV through VI in monkeys[17]. Axons of LCN neurons project to the contralateral thalamus and terminate primarily in the ventral posterior lateral (VPL) and posterior nuclei. There is also a small projection to the central lateral nucleus (CL) in monkey, but not in cat[5,10,11,18,19,22,32,33,36,44]. Projections from LCN to the mesencephalon have been demonstrated in monkey, cat and rat[6,28,43,48,52,56,57]. Smaller projections have been shown to the dorsal and medial nuclei of the accessory olive[7,36,46,47]; medial reticular formation[48]; and to caudal portions of the spinal cord[27].

The number of cells in LCN varies among species[4,12,20,28,29,40,45]. The LCN is present in monkeys and other primates[17,20,25,35,45,52], however, there is discrepancy as to the size, or even the existence of LCN in humans[35,39,54]. Thalamically projecting LCN neurons have not been systematically investigated in primates. In this study we report the number, location and morphology of thalamically projecting LCN neurons and compare them to the total population of LCN cells in the monkey. These results have been presented in abstract form[50].

MATERIALS AND METHODS

Nine monkeys were used in this study. Six monkeys (4 *Macaca fascicularis*, MF 1–4, 2.0–3.5 kg, and two *Saimiri sciureus*, SQ1–2, 0.6–1.4 kg) received thalamic horseradish peroxidase (HRP) injections to study LCN neurons with terminations in the thalamus. Cervical spinal tissue, cut in cross section, was examined in 3 *Macaca fascicularis* (MF 10–12), using Nissl stain to determine the total number of cells in LCN. Animals MF1–4 and SQ1–2 were also used in prior studies of the spinothalamic tract[2,3]. Details of the HRP injections, tissue processing, and data collection are described in those papers. The criteria for selecting the 6 animals used were: (1) adequate placement of HRP within somatosensory regions of the thalamus and (2) no fading of HRP reaction product in the spinal cord. HRP-processed tissue used in this study was analyzed a few weeks to many months (maximum 1 year), after initial tissue processing. To assure that the number of HRP-labeled cells seen had not faded over time, all tissue was examined and compared to prior counts of spinothalamic cells in the gray matter. There was no significant change in the number of HRP-labeled spinal cord cells in tissue from animals used in this study when compared to counts from the initial study. Some animals were rejected from the present study due to fading of the HRP reaction product over time. Some of the monkeys used in this study also received white matter lesions of the mid-thoracic spinal cord as part of the initial study.

The borders of the upper cervical segments were defined as

Correspondence: A. Vania Apkarian, Neurosurgery Research Laboratories, SUNY Health Science Center, 766 Irving Avenue, 3118 Weiskotten Hall, Syracuse, NY 13210, U.S.A. Fax: (1) (315) 464-5520.

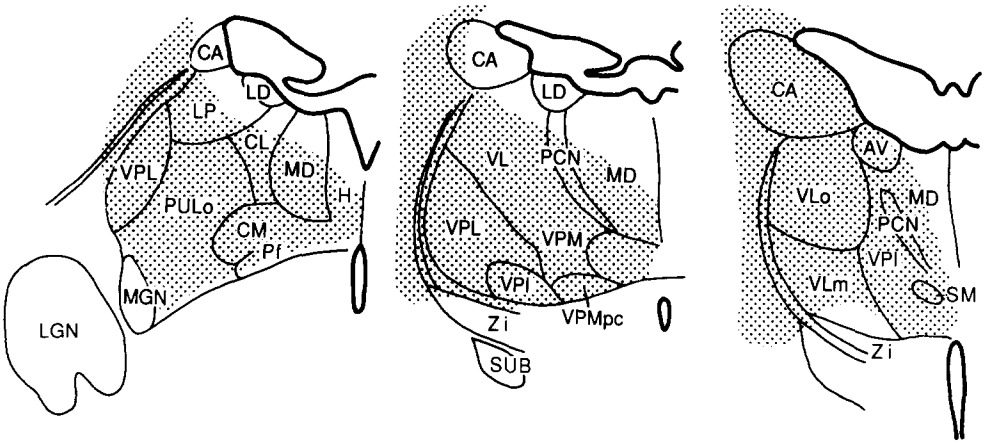

Fig. 1. Drawings of the extent of the HRP injection site for squirrel monkey SQ1 (from Apkarian and Hodge[2], used with permission). The levels represented correspond to: the posterior most region of VPL, the middle region of VPL, and the region of the oralis division of the ventral lateral nucleus (VLo). The nomenclature is adapted from Emmers and Akert[26]. Labels of nuclei are as follows: AV, anterior ventral; CA, caudate; CL, central lateral; CM, center median; H, habenula; LD, lateral dorsal; LGN, lateral geniculate; LP, lateral posterior; MGN, medial geniculate; PCN, paracentral; Pf, parafascicular; PULo, pulvinar oralis; SUB, substantia nigra; VL, ventral lateral; VPI, ventral posterior inferior; VPL, ventral posterior lateral; VPMpc, parvocellular division of ventral posterior medial; Zi, zona incerta.

follows: the medullary–C1 junction was the last microscopic section in which the gray matter was broken up by the decussation of the pyramids. The C1–C2 junction was the most rostral C2 dorsal rootlet, grossly. The C2–C3 and C3–C4 junctions were the midpoints between the two groups of dorsal rootlets, grossly.

Cells labeled with HRP were examined using brightfield and darkfield microscopy. Alternate sections from the mid-medulla to C3, and in some cases to C4, were analyzed. The number of HRP-labeled LCN cells were recorded for each section and the number of labeled cells per millimeter length of spinal cord computed (computations based on 60-μm sections for macaques and 80-μm sections for squirrel monkeys). To minimize repeated counting only cells with well defined nuclei were counted. Locations of labeled LCN cells were plotted using potentiometers attached to the microscope stage, and connected to a Zenith AT computer (Minnesota Datametrics Corp.). The plotting accuracy of this system is 5 μm.

Cell diameters of labeled LCN cells were entered into a PDP11/34 computer using a digitizing tablet. The tablet cursor was viewed simultaneously with the microscope image (at 400×) through a drawing tube. Two distances corresponding to the long and short perpendicular axes of the cell, as determined by the boundary of HRP reaction product, were entered through the tablet. These two values were averaged to determine an estimated diameter for each cell, and were also used to generate scattergrams of cell shapes. The scattergrams consist of single points representing individual cells where the length of the long axis of each cell is plotted on the ordinate and the length of the short axis on the abscissa. Cell diameter and shape measurements were done only on cells with a clear nucleus or, in cases where the labeling was dense enough to obscure the nucleus, only when obvious dendritic profiles were seen extending from the soma. The resolution of this system has been determined to be in the range of one μm (ref. 3).

Statistical analysis was used to test changes in cell diameter and shape along the rostro-caudal extent of the nucleus. The ratio of the longest and shortest axis for each cell was used as a measure of cell shape. The analysis was performed by grouping labeled LCN cells by spinal segment (medulla, C1, C2, and C3) and applying analysis of variance. If the analysis of variance was significant ($P < 0.05$), Tukey's criterion for multiple comparison, using a two-tailed t-test,

TABLE I

Thalamically projecting LCN cells (A) and total LCN cells in Nissl-stained tissue (B)

EXP	*MED*	*C1*	*C2*	*C3r*	*C3c*	*C4*	*Total*	*Adjusted total*
A								
MF1	10*	233	97	22	0	0	600**	462$
MF2	22	128	129	13	0	0	525	404
MF3	38	106	19	11	6	0	350	270
MF4	7	135	85	–	–	–	>500	>385
SQ1	22	112	62	23	–	–	550	451
SQ2	8	102	54	21	2	–	N.D.	N.D.
B								
MF10	90	167	162	61	83	72	1250	918
MF11	65	62	163	89	88	49	950	697
MF12	167	255	320	194	67	29	2650	1945

* number of cells per mm of spinal cord tissue, ** calculated total cells in LCN in each animal, $ adjusted total counts using a mean cell diameter of 18 μm and appropriate section thicknesses, N.D., not determinable; –, tissue not available.

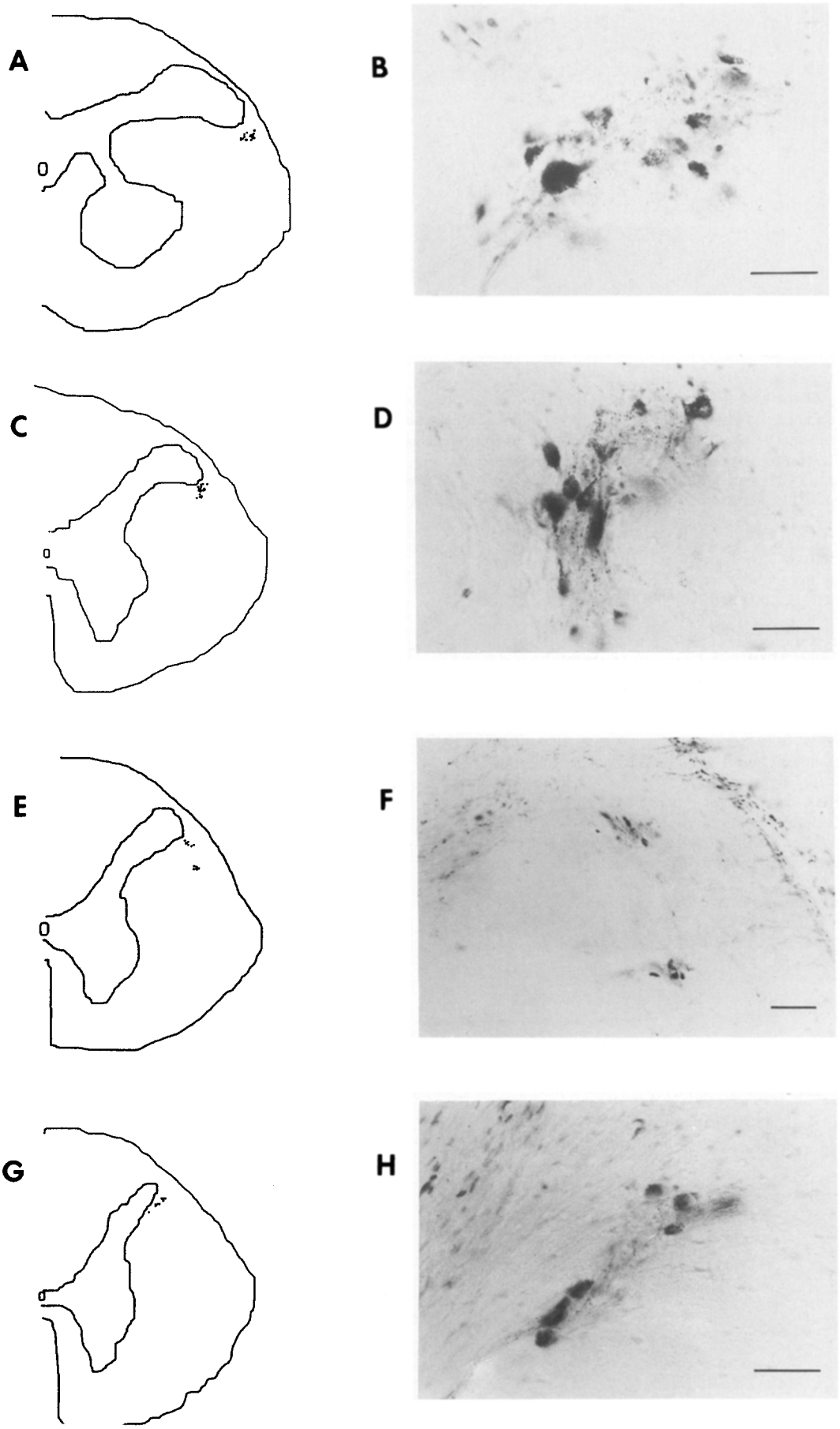
A
B
C
D
E
F
G
H

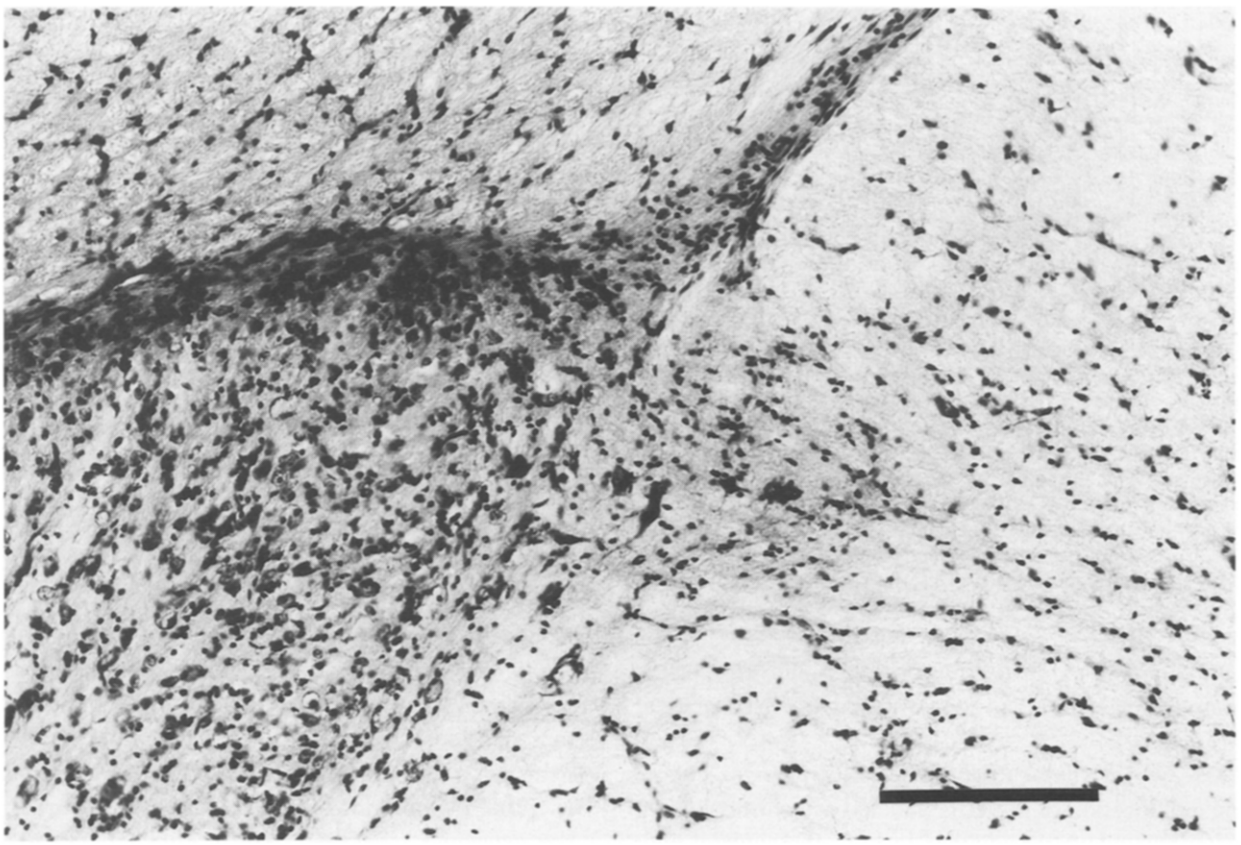

Fig. 3. Photomicrograph of LCN neurons in C4. Cresyl violet-stained cross section from monkey MF11. The clump of large cells just outside the gray matter are LCN cells located in C4. Boundaries of the dorsal horn are seen to the left, dorsal is up, medial is left. Bar = 200 μm.

was used to test significance between all combinations of groups[51]. A joint significance of $P < 0.05$ was required for significance. Numbers are reported as mean ± standard deviation.

Three deeply anesthetized macaques (MF 10–12) were perfused with 4% paraformaldehyde, the medulla to C4 was cut in cross section (50 μm), and the tissues stained with Cresyl violet. All LCN cells on one side of the spinal cord were counted in alternate sections to estimate the total number of LCN cells.

RESULTS

Injection sites

The injection sites for each of the 6 monkeys studied (macaques MF1, MF2, MF3, and MF4, and squirrel monkeys SQ1 and SQ2) adequately covered the medial and lateral somatosensory areas of the thalamus unilaterally and did not spread into the midbrain. An example of the injection site for monkey SQ1 is shown in Fig. 1 (injection sites for all the monkeys are in Fig. 1 of each paper by Apkarian and Hodge[2,3] where MF1–MF4 are referred to as MFV1, MF1, MFD2, and MFD3; and SQ1 and SQ2 as SQV1 and SQD3, respectively).

Morphology of the lateral cervical nucleus projecting to the thalamus

The borders of LCN were better demarcated in the HRP-reacted tissue than in Nissl-stained sections. Likewise, somatic structures were better visualized in the HRP-reacted tissue. Therefore, nucleus boundaries and cell morphology were studied only in HRP preparations. LCN cells were defined as those clearly lying in the white matter of the dorsolateral funiculus. Within the upper cervical spinal cord, the reticulated portion of lamina V extends into the dorsolateral funiculus[3]. Reticulated lamina V cells were not considered part of LCN. LCN cells were also defined by their characteristic shapes (they tended to be more round, and more heavily labeled with

←

Fig. 2. Characteristic changes in the shape and location of the lateral cervical nucleus as determined by HRP-labeled cells following thalamic injection. A and B are from rostral C1; C and D are from rostral C2; E and F are from mid C2; G and H are from rostral C3; in one squirrel monkey (SQ1). Drawings on the left show positions of labeled cells in relation to the spinal cord gray matter. Photographs on the right are of HRP-labeled LCN cells from the same section as shown on the left. Notice the fine speckling of HRP-filled processes around the labeled LCN cells; this is best seen in D. Bar = 50 μm in B, D, and H, and 100 μm in F.

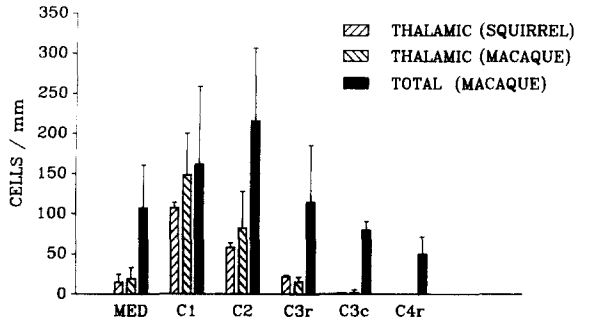

Fig. 4. The average number of LCN cells per millimeter length of spinal cord for each spinal segment from the medulla to C4. The rostral and caudal halves of the third cervical segment (C3r and C3c) are graphed separately. Each bar represents the average of all animals in a group. Error bars represent the standard deviations of the means. Right diagonal bars represent thalamically projecting cells in animals MF1–4 (thalamic (macaque)), left diagonal bars represent thalamically projecting cells in animals SQ1–2 (thalamic (squirrel)). Solid bars indicate the numbers of the total LCN cells (Nissl-stained) in animals MF10–12 (total (macaque)).

HRP in comparison to dorsal horn cells) and were often surrounded by HRP-filled processes suggestive of labeled axons (Fig. 2).

There was a characteristic pattern of changes in the shape and location of the HRP-labeled cell clusters along the neuraxis which was similar in both the squirrel and macaque monkeys (Fig. 2). In the medulla and upper C1, HRP-labeled LCN cells formed a tight group just off the tip of the dorsal horn (Fig. 2A,B). In lower C1 and C2 these cells extended further out into the ventrolateral white matter and often broke up into two or more islands of cells (Fig. 2C–F). In C3 the HRP-labeled cells were located more medially and oriented parallel to, and abutting the lateral border of the dorsal horn. Here the cells were more fusiform and were located close to dorsal horn lamina I cells (Fig. 2G,H). Labeled cells in ventral C3 were usually more fusiform in shape than those in dorsal C3. To minimize counting lamina I cells as being in LCN, cells in this region were counted as LCN neurons only if they were clearly in the white matter.

The morphology and location of the LCN as seen in Nissl-stained preparations was similar to that of the thalamically projecting subset of the nucleus. In C4, LCN neurons were seen in the Nissl-stained preparations only (Fig. 3). The morphology, and location within the white matter of these C4 LCN cells was similar to HRP-labeled cells in C3. In 3 animals (1 macaque and 2 squirrel monkeys) the dorsolateral white matter of the cervical enlargement was examined in Nissl material. A small number of cells were observed in this region (about 15 cells/mm); however, most of these cells were of variable shape, size and position, rendering them indistinguishable from lamina I or reticulated V neurons displaced to the immediately adjacent white matter.

Cell counts

The average number of thalamically projecting LCN cells was 506 ± 94 (n = 5), unilaterally (Table I). Only random sections were available for SQ2, therefore, no estimate of the size of the total projection was possible for this animal. Table I also provides adjusted total counts (using Abercrombie's correction factor[1] and a mean cell diameter of 18 μm) that estimate the mimimum total counts. Since every effort was made not to count cell fragments (for cell counting details see Apkarian and Hodge[3]), the unadjusted counts are more reflective of the true numbers of LCN cells projecting to the thalamus. The first cervical segment contained the highest concentration of labeled LCN cells (cells/millimeter length of spinal cord) in all cases except MF2 where the concentration of LCN cells was nearly equal in C1 and C2 (Table I). However, the total number of cells found in C2 was approximately equal to the total number in C1 in macaques. This difference is due to the short length of the C1 segment. The average length of each spinal segment in the 4 macaques with HRP injections was: 1.05 mm in the lower medulla (an area where LCN type neurons were clearly visible), 1.44 mm in C1, 3.15 mm in C2, and 3.48 mm in C3 (rostral and caudal portions). In the macaques (averaged over 4 animals), 4% of HRP-labeled cells were in the medulla, 44% in C1, 47% in C2, and 5% in C3; while in the squirrel monkeys (averaged over 2 animals), 6% of HRP-labeled cells were in the medulla, 52% in C1, 35% in C2, and 7% in C3. Only in one of the 6 animals (MF3) were HRP-labeled LCN cells found in the caudal half of C3. Spinal segment C4 was analyzed in 4 of the 6 animals and in no cases were any HRP-labeled LCN cells found. There was significant section-to-section variation in the number of LCN cells counted in all animals studied. The range of ipsilaterally projecting LCN cells was 0–15 per animal.

The total number of LCN cells in Nissl-stained experiments was 1617 ± 908 (MF10–12, see Table I). Table I also provides adjusted total counts that estimate the minumum total counts of LCN cells. Again, the unadjusted counts are thought to be more reflective of the total number of LCN cells (vide supra). In all 3 animals LCN cells were found from the medulla down to the C4 segment. The highest concentration of LCN cells was in C2 (Table I). In these animals 5% of all Nissl-stained LCN cells were located in the medulla, 15% in C1, 53% in C2, 22% in C3, and 4% in rostral C4. The average length of spinal tissue examined in these 3 animals was 0.6 mm in the medulla, 1.24 mm in C1, 3.03 mm in C2, 2.96 mm in C3 and 1.2 mm in rostral C4. The rostro-caudal distribution of Nissl-stained LCN neurons (total LCN) and HRP-labelled cells (thalamic projection from LCN) is shown in Fig. 4. This figure illustrates that

thalamically projecting LCN cells constitute a rostrally located subpopulation of the nucleus.

Morphology of LCN cells projecting to the thalamus

Cell diameters were collected in two animals: MF1 and SQ1. The estimated cell diameter (long axis/2 + short axis/2) and cell axes ratio (long axis/short axis) were computed for each HRP-labeled cell, and the mean and standard deviation determined for each spinal segment. The average cell diameter of thalamically projecting LCN cells decreased in more caudal portions of the nucleus (Fig. 5A,C,E and G). The average estimated diameters of labeled LCN cells in MF1 were: 23.1 μm in the medulla (n = 3), 18.6 μm in C1 (n = 79), 16.7 μm in C2 (n = 35), and 13.8 μm in C3 (n = 9). For SQ1 the averages were: 16.7 μm in the medulla (n = 10), 15.6 μm in C1 (n = 73), 13.5 μm in C2 (n = 45), and 14.4 μm in C3 (n = 7). Analysis of variance showed a significant relationship between cell size and spinal segment for each animal separately (F = 8.05, df = 3,122 for MF1; F = 10.09, df = 3,131 for SQ1). Using Tukey's criterion for multiple comparison, the following pairs were found to have significantly smaller cells in the caudal segment: C1–C2, C1–C3, medulla–C2, and medulla–C3 for MF1; and C1–C2, and medulla–C2 for SQ1.

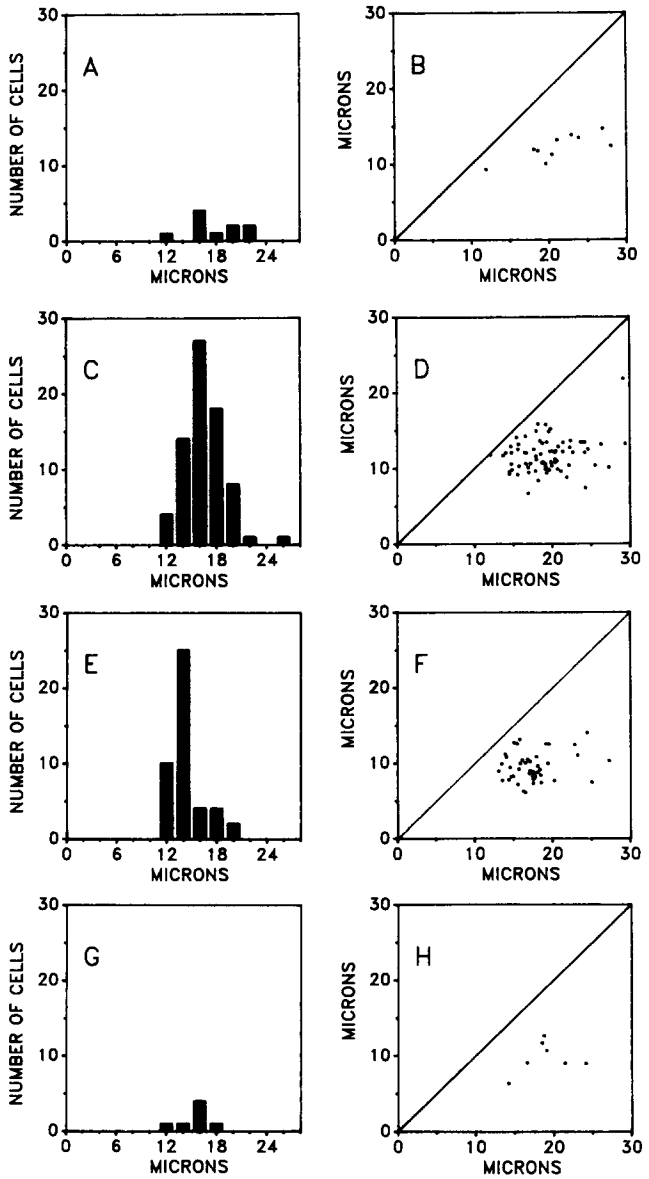

Fig. 5. Distribution of size and shape of labeled LCN cells in one squirrel monkey (SQ1). Left column: histograms of the cell diameter of HRP-labeled LCN cells in the upper medulla (A), C1 (C), C2 (E), and C3 (G). Binwidth = 2 μm. Right column: scattergrams of neuronal shapes for HRP-labeled LCN cells in the upper medulla (B), C1 (D), C2 (F), and C3 (H). Each point on the scattergram corresponds to a labeled cell such that the position along the abscissa corresponds to the length of the larger axis of the cell and the position along the ordinate corresponds to the smaller axis. The degree of cell skewness can be determined for a particular cell on the scattergram by drawing a line from the origin to the point representing that cell and measuring the angle between it and the X axis. The smaller the angle, the more skew the cell, i.e., the more oblong in shape; the larger the angle, the more round the cell. Round cells would be located on the 45 °C line. Larger cells are farther from the origin than smaller ones.

Scattergram plots of cell shapes (Fig. 5B,D,F, and H) revealed that thalamically projecting LCN cells become more fusiform in shape in more caudal portions of the nucleus. The average cell axes ratios for MF1 were: 1.52 in the medulla, 1.74 in C1, 1.61 in C2, and 2.51 in C3. For SQ1 the average cell axes ratios were: 1.72 in the medulla, 1.69 in C1, 1.91 in C2, and 1.99 in C3. Analysis of variance of the cell axes ratios showed a significant relationship between cell shape and spinal segment (F = 6.64, df = 3, 122 for MF1; F = 3.20, df = 3, 131 for SQ1). Using Tukey's criterion the following pairs were found to have significantly more fusiform cells in the more caudal sections: medulla–C3, C1–C3, and C2–C3 for MF1; and C1–C2 for SQ1.

DISCUSSION

These experiments represent the first quantitative study of the thalamically projecting LCN cells in primates. The number of thalamically projecting LCN cells and their distribution along the neuraxis was similar in both species studied. The total number of LCN cells projecting to the contralateral thalamus was approximately 500. The total number of LCN cells was approximately 1600, determined in Nissl material. These counts indicate that about one-third of primate LCN cells project to the thalamus. The thalamically projecting LCN cells were found in the rostral portion of LCN. The morphology and size of thalamically projecting LCN cells varied along the rostro-caudal extent of the nucleus. The shape and relative location of the LCN within the white matter also varied along its rostro-caudal extent. These rostro-caudal changes were similar to previous descrip-

tions of LCN in cat[22,49] and monkey[8,12], with the exception that LCN is smaller and closer to the dorsal horn in monkeys than it is in cats[8,12]. Our results differ from other reports in monkey[8,12,20,45], and cat[22,49] since we describe LCN cells extending into C4. Within the cervical enlargement, a small inhomogeneous group of cells were also observed in the dorsolateral white matter. The LCN in rat has a more limited extent than in other species since it is found primarily in C2[4,12,43]. Cells in the dorsolateral white matter in the rat have been subdivided into cervical (LCN) and spinal (LSN) components based on location, morphology, supraspinal projections, immunocytochemistry and physiology[31]. Whether a similar subclassification should be used in the monkey remains to be determined.

Boivie[12] studied LCN in a number of primate species, including macaque and squirrel monkeys. Using Cresyl violet stain, he found 'less than 2000' cells on one side which closely agrees with our results. Using retrograde transport of HRP, however, he estimated that 'slightly higher numbers' of labeled LCN cells could be seen as compared to the LCN cells in Cresyl violet-stained tissue. Although Boivie implies larger numbers of thalamically projecting LCN cells than reported here, his estimates are not based on systematic counts (Boivie, J., personal communication), the size and placement of the HRP injection sites was not reported, and the region of spinal cord examined is unknown (in C1 the number of HRP-labeled cells is nearly equal to the total number; see Fig. 4). Trevino[52] showed LCN cells labeled with HRP in two monkeys. One animal had injections in the lateral thalamus, the second animal had injections centered in the periaqueductal gray. Although the labeled cells illustrated in C2 in both animals seem similar in number, the data were not quantified.

It is possible that more LCN cells may have been labeled if another tracer had been used. For example, Lima and Coimbra[41] found many more rat spinothalamic cells labeled when choleratoxin subunit B was used instead of HRP. However, using choleratoxin subunit B does not increase the numbers of labeled LCN cells as compared to HRP in cat[28]. As reported by other investigators[12,22], the exact borders of LCN in the medulla were difficult to delineate in both Nissl-stained and HRP-labeled tissue due to the large numbers of cells surrounding LCN in this region; hence only caudal medullary sections were analyzed. Some lamina I spinothalamic neurons could have been confused with thalamically projecting LCN cells because HRP-labeled LCN cells are located just lateral to the dorsal horn gray matter, especially in C3. However, lamina I spinothalamic cells in C2 have been shown to be more oblong and smaller than the thalamically projecting LCN cells in this region in the monkey (compare Fig. 5 to Figs. 21 and 22 of Apkarian and Hodge[3]). The same also holds true for cells in C3. These morphologic differences indicate that few if any lamina I cells were included in the counts of neurons in the LCN.

Cell diameters of LCN cells have been reported earlier[12,20,22,40,45,54]. It has been the experience of this laboratory that cell diameter measurements can vary widely between animals[3], and therefore, no attempt will be made to compare cell diameter values to other reports. What can be learned from the cell diameter data is that thalamically projecting LCN cell somas are smaller in size and more oblong in shape in more caudal regions of the spinal cord. It is likely that similar changes occur in other species since the presence of more than one cell shape is commonly mentioned[20,22,45,49,54,55]. The scattergrams indicate that the cell shapes do not fall into particular groups such as round, or fusiform, but rather that they form a continuum. Craig and Burton[22] reported that small cells were concentrated in the medial one-third of the feline LCN, but made no rostro-caudal distinction in changes in cell sizes.

The number of thalamically projecting LCN cells in monkey is much less than that reported in the cat. In cats, the total number of LCN cells have been reported to range from 6300 to 9100, and 91–97% of these project to the thalamus (see Table I in Flink and Westman[28]). The number of thalamically projecting LCN cells in the monkey are similar to that reported in the rat (approximately 400 cells[4,34]), but greater than that found in the mouse (approximately 250), rabbit (25–150) and guinea pig (100–200)[29]. It should be noted that lower estimates have also been reported for cat and rat[9,22,38]. Unlike other primates, there is a large individual variation in the size of LCN in human tissue where reported counts range between 0 to nearly 4000 cells on one side[53,54].

Wiberg et al. found between 1205 and 2080 labeled LCN cells in macaques (values calculated from Table 4 of Wiberg et al.[57]), following an injection of HRP into the contralateral upper mesencephalic tectum. They also found that approximately one-fourth as many LCN cells were labeled on the ipsilateral side. Since the experimental procedure used by Wiberg et al. is similar to ours (same tracer, comparable survival times and injection sizes, and TMB reaction) the differences in the number of labeled LCN cells between the studies is unlikely to be due to technical differences, especially since the number of HRP-labeled cells in the upper cervical spinal cord is much larger in our study[3] as compared to theirs[57]. Rather the differences most likely reflect underlying anatomy and imply that the LCN-mesencephalic projection is larger than the LCN-thalamic projection in monkeys. Using the results of Wiberg et al.[57], we estimate that

nearly all LCN cells project to the mesencephalon, while only 31% of LCN cells project to the thalamus. In contrast, cats have a heavier LCN projection to the thalamus than to the midbrain[6,9,28]. Flink and Westman[28] report that in cat, 25–49% of LCN cells project to the contralateral tectum and 91–97% project to the contralateral thalamus. Retrograde double labeling studies with fluorescent dyes[6] have shown that 39–48% of the cat LCN cells project to both the thalamus and the tectum, while 8–16% project only to the tectum, and 36–53% project only to the thalamus.

In conclusion, this study proposes that the major projection from LCN in monkey is not to the thalamus, as has generally been assumed[12]. Rather, there are striking differences between cat and monkey in both the size, and the primary efferent targets of LCN. In cat, LCN is relatively large with a dominant projection to the thalamus and a smaller projection to the midbrain; whereas LCN is smaller in monkey with a dominant projection to the midbrain and a smaller projection to the thalamus. Besides differences in termination sites, anatomical and physiological studies have shown differences in LCN inputs between cat and monkey. A higher incidence of nociceptive responsive units are reported in the monkey LCN[25] than in the cat LCN with intact descending inputs[24,37]. Also, immunohistochemical studies show differences in the organization of peptidergic[13] and serotonergic[14] inputs to the LCN between cats and monkeys. Whether these differences relate to functional variations remains to be determined.

Acknowledgements. The authors wish to thank Norma J. Horton and George L. Stanley, Jr. for their technical assistance. This work was supported by NINCDS fellowship number NS08462 (to M.V.S.); NINCDS Grant number NS228910; the Perkins Foundation and a gift from Bristol Laboratories.

ABBREVIATIONS

CL	central lateral nucleus
CM	centre median nucleus
HRP	horseradish peroxidase
LCN	lateral cervical nucleus
MD	medial dorsal nucleus
MED	medulla
MF	*Macaca fascicularis* (macaque monkey)
SM	submedius nucleus
SQ	*Saimiri sciureus* (squirrel monkey)
VPL	ventral posterior lateral nucleus

REFERENCES

1 Abercrombie, M., Estimation of nuclear population from microtome sections, *Anat. Rec.*, 94 (1966) 239–247.
2 Apkarian, A.V. and Hodge, C.J., The primate spinothalamic pathways: II. The cells of origin of the dorsolateral and ventral spinothalamic pathways, *J. Comp. Neurol.*, 288 (1989) 474–492.
3 Apkarian, A.V. and Hodge, C.J., The primate spinothalamic pathways: I. A quantitative study of the cells of origin of the spinothalamic pathway, *J. Comp. Neurol.*, 288 (1989) 447–473.
4 Baker, M.L. and Giesler, G.J., Jr., Anatomical studies of the spinocervical tract of the rat, *Somatosens. Res.*, 2 (1984) 1–18.
5 Berkley, K.J., Spatial relationships between the terminations of somatic sensory and motor pathways in the rostral brainstem of cats and monkeys. I. Ascending somatic sensory inputs to lateral diencephalon, *J. Comp. Neurol.*, 193 (1980) 283–317.
6 Berkley, K.J., Blomqvist, A., Pelt, A. and Flink, R., Differences in the collateralization of neuronal projections from the dorsal column nuclei and lateral cervical nucleus to the thalamus and tectum in the cat: an anatomical study using two different double-labeling techniques, *Brain Research*, 202 (1980) 273–290.
7 Berkley, K.J. and Worden, I.G., Projections to the inferior olive of the cat. I. Comparisons of input from the dorsal column nuclei, the lateral cervical nucleus, the spino-olivary pathways, the cerebral cortex and the cerebellum, *J. Comp. Neurol.*, 180 (1978) 237–252.
8 Björkland, M. and Boivie, J., Lateral cervical nucleus of monkey and its projection to the thalamus, *Neuroscience*, 7 (1982) s487–s487. (Abstract.).
9 Blomqvist, A., Flink, R., Bowsher, D., Griph, S. and Westman, J., Tectal and thalamic projections of dorsal column and lateral cervical nuclei: a quantitative study in the cat, *Brain Research*, 141 (1978) 335–341.
10 Boivie, J., The termination of the cervicothalamic tract in the cat. An experimental study with silver impregnation methods, *Brain Research*, 19 (1970) 333–360.
11 Boivie, J., Thalamic projections from lateral cervical nucleus in monkey. A degeneration study,, *Brain Research*, 198 (1980) 13–26.
12 Boivie, J., Anatomic and physiologic features of the spinocervico-thalamic pathway. In G.A. Rustioni, and R. Spreafico Macchi (Eds.), *Somatosensory Integration in the Thalamus*, Elsevier, Amsterdam, 1983, pp. 63–106.
13 Broman, J. and Blomqvist, A., Substance P-like immunoreactivity in the lateral cervical nucleus of the owl monkey (*Aotus trivirgatus*): a comparison with the cat and rat, *J. Comp. Neurol.*, 289 (1989) 111–117.
14 Broman, J. and Blomqvist, A., Serotonergic innervation of the lateral cervical nucleus: an immunohistochemical study in cats and monkeys (*Aotus trivirgatus*), *Synapse*, 6 (1990) 55–62.
15 Brown, A.G. and Franz, D.N., Responses of spinocervical tract neurones to natural stimulation of identified cutaneous receptors, *Exp. Brain Res.*, 7 (1969) 231–249.
16 Brown, A.G., Fyffe, R.E.W., Noble, R., Rose, P.K. and Snow, P.J., The density, distribution and topographical organization of spinocervical tract neurones in the cat, *J. Physiol.*, 300 (1980) 409–428.
17 Bryan, R.N., Coulter, J.D. and Willis, W.D., Cells of origin of the spinocervical tract in the monkey, *Exp. Neurol.*, 42 (1974) 574–586.
18 Carstens, E. and Trevino, D.L., Anatomical and physiological properties of ipsilaterally projecting spinothalamic neurons in the second cervical segment of the cat's spinal cord, *J. Comp. Neurol.*, 182 (1978) 167–184.
19 Carstens, E. and Trevino, D.L., Laminar origins of spinothalamic projections in the cat as determined by the retrograde transport of horseradish peroxidase, *J. Comp. Neurol.*, 182 (1978) 151–166.
20 Chen, Z.-Y., Jou, T.-C. and Tsai, T., Experimental studies on the nucleus cervical lateralis (NCL) of *Macaca cyclopis* (Swinhoe). Part I: The general morphology and the spinal cord origins of the nucleus cervicalis lateralis of the monkey (Macaca cyclopis), *J. Formosan. Med. Assoc.*, 70 (1971) 453–467.
21 Craig, A.D., Jr., Spinal and medullary input to the lateral

cervical nucleus, *J. Comp. Neurol.*, 181 (1978) 729–744.
22 Craig, A.D., Jr. and Burton, H., The lateral cervical nucleus in the cat: anatomic organization of cervicothalamic neurons, *J. Comp. Neurol.*, 185 (1979) 329–346.
23 Craig, A.D., Jr., Sailer, S. and Kniffki, K.-D., Organization of anterogradely labeled spinocervical tract terminations in the lateral cervical nucleus of the cat, *J. Comp. Neurol.*, 263 (1987) 214–222.
24 Craig, A.D., Jr. and Tapper, D.N., Lateral cervical nucleus in the cat: functional organization and characteristics, *J. Neurophysiol.*, 41 (1978) 1511–1534.
25 Downie, J.W., Ferrington, D.G., Sorkin, L.S. and Willis, W.D., Jr., The primate spinocervicothalamic pathway: responses of cells of the lateral cervical nucleus and spinocervical tract to innocuous and noxious stimuli, *J. Neurophysiol.*, 59 (1988) 861–885.
26 Emmers, R. and Akert, K., *A Stereotaxic Atlas of the Brain of the Squirrel Monkey (Saimiri Sciureus)*, University of Wisconsin Press, Madison, Wisconsin, 1963.
27 Flink, R. and Svensson, B.A., Fluorescent double-labelling study of ascending and descending neurones in the feline lateral cervical nucleus, *Exp. Brain Res.*, 62 (1986) 479–485.
28 Flink, R. and Westman, J., Different neuron populations in the feline lateral cervical nucleus: a light and electron microscopic study with the retrograde axonal transport technique, *J. Comp. Neurol.*, 250 (1986) 265–281.
29 Giesler, G.J., Miller, L.R., Madsen, A.M. and Katter, J.T., Evidence for the existence of a lateral cervical nucleus in mice, guinea pigs, and rabbits, *J. Comp. Neurol.*, 263 (1987) 106–112.
30 Giesler, G.J., Jr., Björkland, M., Xu, Q. and Grant, G., Organization of the spinocervicothalamic pathway in the rat, *J. Comp. Neurol.*, 268 (1988) 223–233.
31 Giesler, G.J., Jr. and Elde, R.P., Immunocytochemical studies of the peptidergic content of fibers and terminals within the lateral spinal and lateral cervical nuclei, *J. Neurosci.*, 5 (1985) 1833–1841.
32 Giesler, G.J., Jr., Menetrey, D. and Basbaum, A.I., Differential origins of spinothalamic tract projections to medial and lateral thalamus in the rat, *J. Comp. Neurol.*, 184 (1979) 107–126.
33 Giesler, G.J., Jr., Urca, G., Cannon, J.T. and Liebeskind, J.C., Response properties of neurones of the lateral cervical nucleus in the rat, *J. Comp. Neurol.*, 186 (1979) 65–78.
34 Granum, S.L., The spinothalamic system of the rat. I. Locations of cells of origin, *J. Comp. Neurol.*, 247 (1986) 159–180.
35 Ha, H. and Morin, F., Comparative anatomical observations of the cervical nucleus, N. cervicalis lateralis, of some primates, *Anat. Rec.*, 148 (1964) 374–375.
36 Horrobin, D.F., The lateral cervical nucleus of the cat: an electrophysiological study, *Q.J. Exp. Physiol.*, 51 (1966) 351–371.
37 Kajander, K.C. and Giesler, G.J., Responses of neurons in the lateral cervical nucleus of the cat to noxious cutaneous stimulation, *J. Neurophysiol.*, 57 (1987) 1686–1704.
38 Kemplay, S.K. and Webster, K.E., A qualitative and quantitative analysis of the distributions of cells in the spinal cord and spinomedullary junction projecting to the thalamus of the rat, *Neuroscience*, 17 (1986) 769–789.
39 Kircher, C. and Ha, H., The nucleus cervicalis lateralis in primates, including the human, *Anat. Rec.*, 160 (1968) 376–376.
40 Kitai, S.T., Ha, H. and Morin, F., Lateral cervical nucleus of the dog: anatomical and microelectrode studies, *Am. J. Physiol.*, 209 (1965) 307–311.
41 Lima, D. and Coimbra, A., The spinothalamic system of the rat: structural types of retrogradely labelled neurons in the marginal zone (lamina I), *Neuroscience*, 27 (1988) 215–230.
42 Lu, G.-W., Spinocervical tract-dorsal column postsynaptic neurons: a double-projection neuronal system, *Somatosens. Motor Res.*, 6 (1989) 445–454.
43 Menétry, D., Chaouch, A., Binder, D. and Besson, J.M., The origin of the spinomesencephalic tract in the rat: an anatomical study using the retrograde transport of horseradish peroxidase, *J. Comp. Neurol.*, 206 (1982) 193–207.
44 Metherate, R.S., Da Costa, D.C.N., Herron, P. and Dykes, R.W. A thalamic terminus of the lateral cervical nucleus: the lateral division of the posterior nuclear group, *J. Neurophysiol.*, 56 (1986) 1498–1520.
45 Mizuno, N., Nakano, K., Imaizumi, M. and Okamoto, M., The lateral cervical nucleus of the Japanese monkey, (*Macaca fuscata*), *J. Comp. Neurol.*, 129 (1967) 375–384.
46 Molinari, H.H., Ascending somatosensory projections to the dorsal accessory olive: an anatomical study in cats, *J. Comp. Neurol.*, 223 (1984) 110–123.
47 Molinari, H.H., Ascending somatosensory projections to the medial accessory portion of the inferior olive: a retrograde study in cats, *J. Comp. Neurol.*, 232 (1985) 523–533.
48 Pechura, C.M. and Liu, R.P.C., Spinal neurons which project to the periaqueductal gray and the medullary reticular formation via axon collaterals: a double-label fluorescence study in the rat, *Brain Research*, 374 (1986) 357–361.
49 Rexed, B. and Brodal, A., The nucleus cervicalis lateralis. A spinocerebellar relay nucleus, *J. Neurophysiol.*, 14 (1951) 399–407.
50 Smith, M.V., Stanley, G.L. and Apkarian, A.V., Thalamically projecting cells of the lateral cervical nucleus in monkey, *Soc. Neurosci. Abstr.*, 15 (1989) 757. (Abstract).
51 Steel, R.G.D. and Torrie, J.H., *Principles and Procedures of Statistics, A Biometrical Approach*, McGraw Hill, New York, 1980.
52 Trevino, D.L., The origin and projections of a spinal nociceptive and thermoreceptive pathway. In Y. Zotterman (Ed.), *Sensory Functions of the Skin in Primates, With Special Reference to Man*, Pergamon, New York, 1976, pp. 367–376.
53 Truex, R., Taylor, M. and Smythe, M., The lateral cervical nucleus of the human spinal cord, *Anat. Rec.*, 160 (1968) 443–443.
54 Truex, R.C., Taylor, M.J. and Smythe, M.Q., The lateral cervical nucleus of cat, dog and man, *J. Comp. Neurol.*, 139 (1970) 93–104.
55 Westman, J., The lateral cervical nucleus in the cat. I. A Golgi study, *Brain Research*, 10 (1968) 352–368.
56 Wiberg, M. and Blomqvist, A., The spinomesencephalic tract in the cat: its cells of origin and termination pattern as demonstrated by the intraaxonal transport method, *Brain Research*, 291 (1984) 1–18.
57 Wiberg, M., Westman, J. and Blomqvist, A., Somatosensory projection to the mesencephalon: an anatomical study in the monkey, *J. Comp. Neurol.*, 264 (1987) 92–117.